Atomic superlattice formation mechanism revealed by scanning tunneling microscopy and kinetic Monte Carlo simulations

X. P. Zhang,[1,2] B. F. Miao,[1] L. Sun,[1] C. L. Gao,[2] An Hu,[1] H. F. Ding,[1,*] and J. Kirschner[2]
[1]*Nanjing National Laboratory of Microstructures and Department of Physics, Nanjing University, 22 Hankou Rd., Nanjing 210093, China*
[2]*Max-Planck-Institute of Microstructure Physics, Weinberg 2, 06120 Halle, Germany*
(Received 9 November 2009; revised manuscript received 2 February 2010; published 26 March 2010)

We study the interaction of single Fe atoms on Cu(111) and Ag(111) substrates with low-temperature scanning tunneling microscopy and kinetic Monte Carlo simulations. In Fe/Cu(111), a self-assembled hexagonal quasisuperlattice with perturbation of around 20% dimers/clusters is obtained. In Fe/Ag(111), however, a disorderlike structure is found even though long-range interactions among atoms are observed. In combination with kinetic Monte Carlo simulations, possible mechanisms of the superstructure formation are discussed. We find that two parameters, i.e., the ratio of adatom interaction energy (the depth of the first energy minimum) to diffusion barrier and the square of the repulsive ring radius versus the superstructure lattice constant, play important roles for superstructure formation.

DOI: 10.1103/PhysRevB.81.125438 PACS number(s): 68.37.Ef, 05.65.+b

I. INTRODUCTION

Magnetic nanostructures have attracted theoretical and experimental interest due to their new physical properties and potential applications.[1–9] With the advance of modern growth and imaging techniques, it is possible to fabricate structures down to the atomic level. Atomic manipulation through scanning tunneling microscopy (STM) provides an interesting way for creating structures in a designed fashion and investigating their physics.[10,11] Alternatively, self-assembly growth is appealing especially for potential applications as the structures can be fabricated more economically and in relatively large-scale homogeneity.[1,5,9] Recently, substrate mediated long-range interactions (LRI) between adatoms were explored to create self-assembled atomic structures.[1,6,9,12] The LRI was first predicted 50 years ago by Koutecký.[13] Later on Grimley, Einstein, and Lau *et al.*, pointed out that it oscillates with a periodicity of half the Fermi wavelength and decays with increasing the interatomic distance.[14–16] The effect was experimentally first visualized by Tsong[17,18] using field ion microscope on Re/W(110). In Lau and Kohn's[15] paper, they also pointed out that the LRI decays less rapidly in the presence of a surface electron band. In 2000, Hyldgaard and Persson[19] investigated the LRI on the noble metal surface through Shockley surface states which locate at the narrow band gap in the center of the first Brillouin zone of the projected bulk band structures. Due to the fact that the LRI has a slower decay in the presence of the surface band and the wavelength of surface states at the Fermi level is generally longer than that of bulk states, the LRI induced by surface states is easier to be observed. Low-temperature STM is utilized to explore the LRI mediated by surface-state electrons on Ag(111) and Cu(111) surfaces.[1,6,12,20] For a recent review, please see Ref. 21. On Cu/Cu(111) and Co/Cu(111), locally ordered structures with sixfold symmetry were observed, while no superlattice was found. On Co/Ag(111), only a disorderlike distribution (has a broad peak at preferred separation but without sixfold symmetry) was reported. Interestingly, at optimal conditions, Ce/Ag(111) and Ce/Cu(111) show a well-ordered hexagonal superlattice up to a few hundred nanometers.[1,20] Even the large in-plane lattice mismatches among both systems have no influence on the good quality of the superlattices. This is due to the fact that long-range interaction is dominant at this diluted region. In the meantime, *ab initio* theory was used to calculate the interaction energy of 3*d* transition-metal atoms on Cu(111) and quantitative agreement with experimental results was obtained.[22] Negulyaev *et al.*,[23] carried out kinetic Monte Carlo (KMC) simulations for the Ce/Ag(111) system and confirmed that surface-state-mediated LRI is the driving force for superlattice formation. They find the formation mechanism for the superlattice to be a delicate balance between the magnitude of the diffusion barrier and the depth of the first local minimum in LRI, and the concentration of deposited adatoms. Hu *et al.*[24] performed similar simulations for Fe/Cu(111) and predicted that a superlattice can also form in the absence of dimer formation. So far, only a few systems were explored and many parameters were proposed to be important for the superlattice formation. Further studies of other systems are required to generate a more general picture for superstructure formation.

In this paper we present the studies of the interaction of Fe adatoms on Cu(111) and Ag(111) surfaces. The Fe atoms are deposited at the temperature where no apparent atom diffusion was found. STM images show that Fe single atoms are randomly distributed on the substrates. In Fe/Cu(111), the Fe adatoms are self-assembled into a hexagonal quasisuperstructure with perturbation of around 20% dimers/clusters after annealing. In Fe/Ag(111), however, only a disorderlike structure is found even though long range interactions among atoms are observed as well. To understand the mechanism of superstructure formation, we compared different experimental systems and carried out KMC simulations. We find that two parameters, i.e., the ratio of adatom interaction energy (the depth of the first energy minimum) to diffusion barrier and the square of repulsive ring radius versus the superstructure lattice constant, play important roles for superstructure formation.

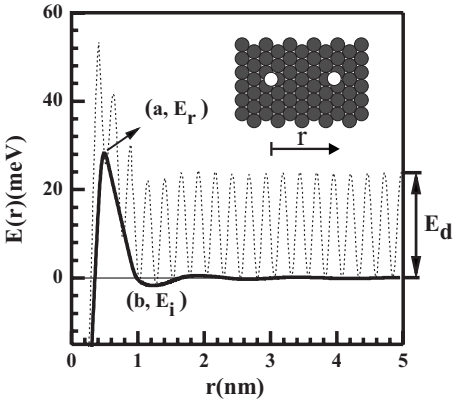

FIG. 1. Superposition (dash line) of the diffusion potential for Fe on Cu(111) and the long-range potential between two atoms mediated by the surface-state electrons (full line). The height of the diffusion potential barrier is 25 meV and the long-range interaction is derived from Ref. 22.

II. EXPERIMENTAL TECHNIQUES

The experiments were carried out in a ultrahigh vacuum low-temperature STM cooled to 4.7 K with base pressure of 5×10^{-11} mbar. The temperature of the STM stage can be accurately controlled by integrated heater and proportional-integral-derivative controller. The single-crystal Cu(111) and Ag(111) substrates are cleaned by repeated cycles of Ar^+ sputtering and annealing to 870 and 970 K, respectively. The clean surfaces with low-impurity concentration are checked by STM. Fe atoms are deposited by means of electron-beam evaporation onto the surfaces of substrates located at the STM stage at 6 K from a thoroughly outgassed Fe rod. The typical rate of deposition is 0.02 monolayer per minute. Electrochemically etched tungsten tips are used for the STM measurements. Bias voltage, V_s refers to the sample voltage with respect to the tip.

III. METHOD OF CALCULATION

We use the KMC method to simulate the growth and annealing process for the formation of the superlattice. The method was used in several systems.[23–25] In the calculations, the difference in fcc and hcp sites is neglected and only hopping between fcc (hcp) sites and the nearest hcp (fcc) sites is taken into account. The hopping rate of an adatom from site i to site j on the (111) surface is calculated using the expression $v_{i-j}=v_0\exp(-E_{ij}/k_BT)$, where T is the temperature of the substrate, v_0 is the attempt frequency, k_B is the Boltzmann's constant and E_{ij} is the hopping barrier, namely, the energy difference between bridge site and initial hollow site. We set v_0 to 10^{12} Hz for Fe atoms on Cu(111) and Ag(111). After LRI is included, the approximate hopping barrier, $E_{ij}=E_d+0.5(E_j-E_i)$, is used, where E_d is the diffusion barrier for an isolated atom on a clean surface, and $E_{i(j)}$ is the total LRI at site $i(j)$.

In the simulations, we use the long-range interaction energy between two Fe atoms mediated by the Cu(111) surface-state electrons calculated by Stepanyuk *et al.*[22] The long-range interaction energy is replotted as a solid line in Fig. 1.

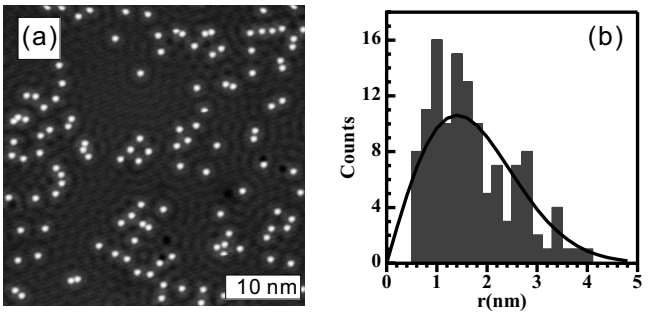

FIG. 2. (a) STM image of ≈0.2% MLE Fe adatoms deposited on Cu(111) at 6 K. (Image size: 40×40 nm^2; sample bias: $V_s=0.1$ V; and tunneling current: $I_t=0.1$ nA). (b) Histogram (bar) of the nearest-neighbor distance obtained from many images like (a) and random distribution (line).

When the two atoms are separated with the lattice constant distance, they form strong chemical bonding, which typically involves the energy on the scale of a few tenths of eV.[26,27] With slightly increasing the separation, the interaction energy enters a repulsive region with the maximum repulsive energy E_r at the separation of a. After that, it encounters its attractive region with the minimum energy E_i at the position b. With further increasing the separation, the interaction oscillates between repulsion and attraction with the period of about half of the Fermi wavelength but with a decreasing amplitude. One should keep in mind that the Fe atoms not only sit on a surface electron sea but also on a hexagonal matrix of atoms. Therefore the Fe atoms have the lowest energy when they sit in the threefold hollow site. When an Fe atom moves from one of this hollow site to a neighboring hollow site, it needs to across an energy barrier (diffusion barrier E_d) as it passes to a bridge position of two Cu atoms. The diffusion barrier for Fe atoms on Cu(111) was estimated to be 25 meV.[8] To present both effects together, we superimpose the diffusion barrier and the long-range interaction potential between two atoms as the dashed line in Fig. 1. We note that the superposition is arbitrary. Due to the existence of the two-dimensional lattice, it does not present the real potential accurately. In our simulations, the real potentials are calculated two dimensionally.

IV. RESULTS AND DISCUSSION

We first investigate the growth of Fe atoms at 6 K. Figure 2(a) shows ≈0.2% monolayer equivalent (MLE) Fe adatoms deposited on Cu(111). The image is obtained with the scanning condition of the sample bias $V_s=0.1$ V and the tunneling current $I_t=0.1$ nA. Most of the Fe's are singles. To obtain the statistics of the interatomic distance, we plot the histogram of the nearest-neighbor separation of the Fe atoms on Fig. 2(b) (bar) and compare to the random distribution function $f_{ran}(r)$ at the given coverage (the solid line). The random distribution function can be derived from a rule of thumb: equal number of atoms occupy equal area. Experimentally, the scanned area typically is a square. To compare with the experimental data, it requires certain correction for the given square shape. The corrected random distribution

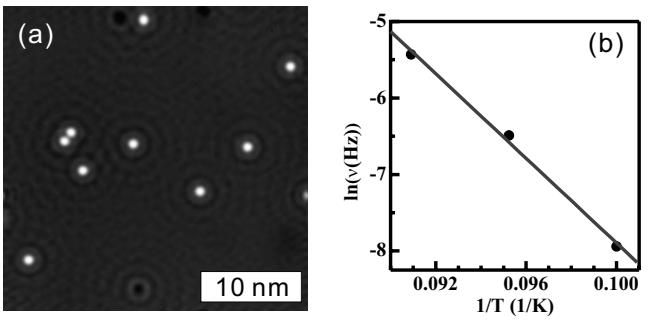

FIG. 3. (a) STM image of ≈0.05% MLE Fe adatoms on Cu (111). (Image size: 30×30 nm^2; sample bias: V_s=0.1 V, and tunneling current: I_t=40 pA). A sequence of images (78 s/frame) at different temperatures is used to derive the Arrhenius plot of the jump rate of isolated Fe monomers (b).

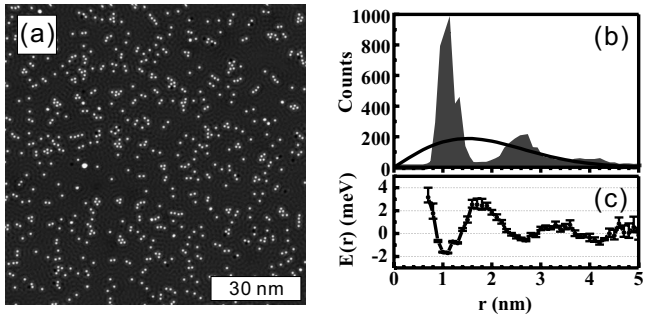

FIG. 4. (a) STM image of 4.2×10^{-3} MLE Fe monomers on Cu (111) obtained after 5 min annealing at 12 K (scan size: 100×100 nm^2; sample bias: V_s=0.1 V; and tunneling current: I_t=0.1 nA). (b) Histogram (bar) from seven images as (a) and the calculated random distribution of the nearest-neighbor distance (line). (c) The long-range interaction energy is derived from (b).

function was previously described by Knorr *et al.*, namely,[6]

$$f_{ran}(r) = (2\pi r\Delta rnN^2/L^2)(1-\pi r^2/L^2)^N \times ([\pi r^2 + (4-\pi)r^2 - 4rL]/\pi L^2),$$

where $L\times L$ is the image size, N is the number of atoms per image and n is the number of images taken into the evaluation. The function has been crosschecked with kinetic Monte Carlo simulations. One can see that the experimental histogram (bar) agrees well with the random distribution function (line) except with $r<0.6$ nm. This suggests that the thermal energy is well below the diffusion barrier E_d and that there is a strong barrier preventing the Fe atom pairs from having a separation of less than 0.6 nm. The Fe atoms also carried some energies when they left the evaporation source, consisting of the thermal energy and the energy carried by Fe ions. This may also influence the distribution. From our experiment, we could not distinguish this influence. This may be due to only a few atoms being deposited and among them only less than 0.1% being ionized.[28]

To characterize the diffusion barrier, we investigate the atomic-diffusion process of single Fe atoms on Cu(111) which are well separated from each other. About 5×10^{-4} MLE Fe atoms are deposited. A typical image is shown in Fig. 3(a). The image is obtained with the scanning condition of the sample bias V_s=0.1 V and the tunneling current I_t =40 pA. Under this condition, we did not find any apparent tip induced atom hopping at 4.6 K. Then the temperature is slowly raised up to temperatures where atomic diffusion can take place within a time period of several minutes to several tens of minutes. Consecutive scanning with the rate of 78 s/frame is carried out to trace single-atom trajectories. The hopping rates at different temperatures are recorded and used to fit with the Arrhenius law $v=v_0\exp(-E_d/k_BT)$ [Fig. 3(b)]. The fitting yields that the diffusion barrier E_d $=23.8\pm1.5$ meV and the attempt frequency $v_0=4\times10^{8\pm1}$. Our measurements agree with previous investigation,[25] where a diffusion barrier $E_d=22\pm7$ meV and the attempt frequency $v_0=1\times10^{10\pm2}$ are obtained. The slight difference may come from the detailed temperature calibration and the tip-induced atom hopping. We note that a previous theoretical calculation yielded the diffusion barrier of 25 meV for Fe atom on Cu(111).[8] The measured diffusion barrier and the attempt frequency also explain why no apparent atomic diffusion was found at 4.6 K.

To explore the long-range interaction among the Fe atoms, we investigate the annealing effect for the samples with different coverage. We found there were noticeable increase in dimer and clusters when the annealing temperature is above 14 K. Therefore, we limit the annealing temperature to be 12 K. Figure 4(a) presents a typical topographic image for the sample with a coverage of 4.2×10^{-3} MLE after annealing at 12 K for 5 min. The image was taken at 4.7 K to avoid the smearing due to the fast movement of atoms. We can see that the Fe atoms tend to keep separate from each other at a preferred distance. At some places, the atoms even form ordered structures. To obtain the quantitative information, we recorded many images and made a histogram of the statistical distribution with the nearest-neighbor Fe separation. The result is shown in Fig. 4(b) as columns. It shows three peaks with decreasing amplitude. The highest peak appears at ≈1.2 nm and the other two peaks at ≈2.7 nm and ≈4.2 nm. The histogram oscillates with a period of 1.5 nm, which is half the wavelength at the Fermi level of the Shockley surface state on Cu(111). The observed histogram is clearly different from the random distribution function at the same coverage (plotted as the solid line in the same figure) which evidences the existence of a long-range interaction among the Fe atoms. To quantify the interaction energy of the long-range interaction, we follow the procedure established by Repp *et al.*[12] and Knorr *et al.*[6] The interaction energy can be obtained through Boltzmann's statistics: $E(r)$ $=-k_BT\ln[f(r)/f_{ran}(r)]$, where $f(r)$ represents the experimental observed histogram and $f_{ran}(r)$ is the random distribution function at the given coverage. Figure 4(c) shows the experimentally determined interaction energy as a function of the adatom separation. We can see that the interaction energy oscillates with decreasing amplitude. The period is about 1.5 nm. The first minimum, which appears at ≈1.1 nm, is about ≈1.7 meV below the energy without any interatomic interaction. The position and amplitude of the energy minimum agree well with the previous experimental investigation[25] and the theoretical calculation by Stepanyuk *et al.*[22]

For a comparison, we performed similar measurements for Fe on Ag(111) system. Our time-dependent hopping rate

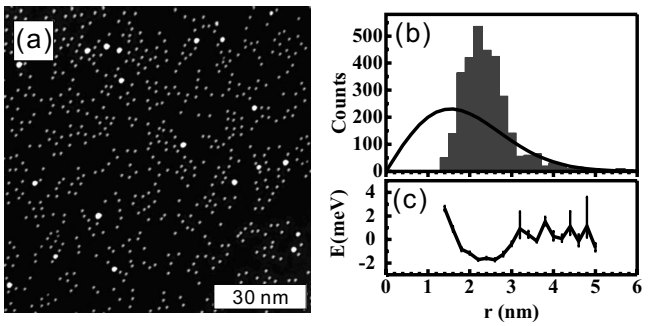

FIG. 5. (a) STM image of 4.7×10^{-3} MLE Fe adatoms on Ag(111) after annealing at 20 K (image size: 100×100 nm^2; sample bias: V_s=0.2 V; and tunneling current: I_t=0.5 nA). (b) Histogram (bar) from (a) and calculated NN distance distribution (line). (c) The calculated interaction energy of Fe atoms on Ag(111).

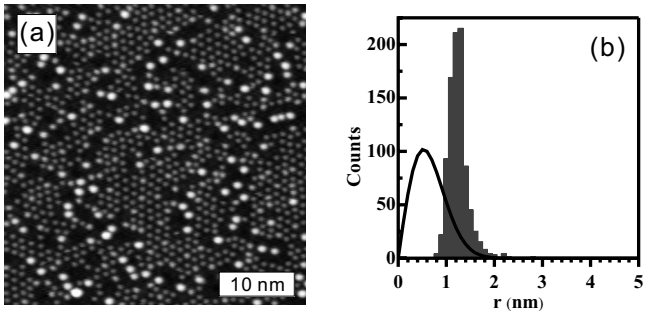

FIG. 6. (a) STM image of Fe quasisuperlattice on Cu(111) after annealing at 12 K, (scan size: 40×40 nm^2; coverage: 4.5×10^{-2} MLE; sample bias: V_s=0.2 V, and tunneling current: I_t=0.5 nA). (b) Histogram (bar) from (a) and the calculated random distribution function of the given coverage (line).

measurements yield the diffusion barrier to be 43.3 ± 4 meV and the attempt frequency to be $1\times10^{12\pm2}$ Hz for Fe atoms on Ag(111). The tunneling conditions of 100 mV and 5 pA are used in the measurement. With this diffusion barrier, a higher temperature, 20 K, is used for the annealing. Figure 5(a) presents a typical image after annealing for 5 min at 20 K. We can see that the Fe atoms seem to be randomly distributed. To obtain more quantitative information, we plot experimentally obtained the nearest-neighbor distribution [bar in Fig. 5(b)] and compare with the random distribution function [line in Fig. 5(b)]. We can see that they are quite different, indicating the presence of the long-range interaction. From the histogram, we calculated the interatomic interaction. The result is shown in Fig. 5(c). We find that the interaction energy of Fe on Ag(111) also oscillates as a function of the interatomic separation. The lowest energy is about $\approx$1.7 meV which is similar to the Fe on Cu(111). The position of the energy minimum, however, appears at a different position, which is around $\approx$2.5 nm for Fe on Ag(111) in contrast to $\approx$1.1 nm for Fe on Cu(111).

Inspired by the work of Silly *et al.*,[1] we try to find the optimum conditions to grow the hexagonal superlattice. As the energy minimum of the long-range interaction energy for Fe/Cu(111) appears at 1.1 nm, we can calculate the optimum coverage for the superlattice to be 4.5×10^{-2} MLE. Therefore, we performed several experiments around this coverage. Figure 6(a) presents the result for coverage θ=4.5 $\times10^{-2}$ MLE. We find that the Fe atoms form a well-ordered hexagonal superlattice except near the white spot region. The white spots are the Fe clusters formed during the growth. Figure 6(b) shows the histogram (bar) obtained from Fig. 6(a). It shows a sharp peak around 1.2 nm. The half width of the peak is about 0.3 nm. For a comparison, the random distribution function is also plotted as a solid line. The peak appears at different position and it is much broader. We also attempted to find the optimum condition for superlattice formation on Fe on Ag(111). However, no matter how we tuned the concentration and the annealing temperature, we did not observe an ordered superlattice. Only disorderlike structures similar to that shown in Fig. 5(a) were obtained.

Comparing Fe on Cu(111) and Ag(111), we find that they are dramatically different even though the interaction energy minimum for both systems is basically the same, i.e., 1.7 meV. The main difference is that we need to use higher temperature to anneal Fe atoms on Ag(111), which is required by the higher diffusion barrier, i.e., $\approx$43 meV vs $\approx$24 meV. Negulyaev *et al.*,[23] pointed out that the formation condition is determined by the subtle balance between the interaction energy and the diffusion barrier. We list the interaction energies, the diffusion barriers, and their ratio for different systems in Table I, including the experiments by Silly, Knorr, Repp, and Negulyaev *et al.*[1,6,12,20] One can find that with decreasing ratio, the ordering of the individual systems becomes worse and worse. For the ratio above 6%, well-ordered or quasiordered superlattices can be obtained for Ce/Ag(111) and Fe/Cu(111). For the ratio around 4%, locally ordered structures but without long-range order can be found for Cu/Cu(111) and Co/Cu(111). For Fe and Co on Ag(111), however, only disorderlike structures are observed.

The physical picture can be understood in the following way: when the atoms are deposited at low temperature, they are randomly distributed on the sample surface as observed in Fig. 2. In order to form an ordered superlattice, the atoms need to make enough steps to hop to the ideal positions. Given the limited experimental time, (5 min in our case), we need to anneal the sample to a temperature where enough hopping could happen. According to the Arrhenius law, the annealing temperature is proportional to the diffusion barrier

TABLE I. Table of the long-range interaction energy and diffusion barrier for different systems.

System	E_i (meV)	E_d (meV)	E_i/E_d (%)	Reference
Ce/Cu(111)	0.9	10	9	20
Ce/Ag(111)	0.8	10	8	1 and 2
Fe/Cu(111)	1.7	23.8	7.1	This work
	1.6	22	7.2	25
Cu/Cu(111)	2.0	40	5.0	6 and 12
Co/Cu(111)	1.6	37	4.2	6 and 29
Fe/Ag(111)	1.7	43.3	3.9	This work
Co/Ag(111)	0.6	40	1.6	6

of the system. Raising of the temperature, however, creates a thermal broadening in the system. The effect of the thermal broadening is determined by the ratio of the depth of the potential well versus the temperature, which is proportional to the interaction energy versus the diffusion barrier. The higher the ratio is, the less the thermal broadening and the better superlattice can be achieved. Therefore, we can conclude that the ratio is one of the critical parameters which determine the formation condition for the superlattice.

One may also notice that there is slight difference between Fe/Cu(111) and Ce/Ag(111) even though they have very similar ratio of interaction energy versus the diffusion barrier. For Ce/Ag(111), an almost perfect superlattice can be achieved. For Fe/Cu(111), however, only a quasisuperlattice is obtained. There are Fe dimers and clusters on the Cu(111) surface as well. It was pointed out that the formation of the dimers and clusters can dramatically influence the formation of the superlattice.[24] Due to the strong chemical bonding (typically one order of magnitude larger than the LRI energy[26,27]), the dimers and clusters are very stable. Once they are formed, it is difficult for them to break up and become monomers again. One can imagine that the dimers and clusters have much higher diffusion barriers than the Fe monomers as the effective mass is bigger. This makes it difficult for them to move to the ideal position for the superlattice which leaves disorder in the system.

From the separation-dependent interaction between Fe atoms on Cu(111), shown in Fig. 1, one can see that the Fe atoms need to pass a repulsive region before forming dimers. There is a critical separation, a with the maximum repulsive energy E_r. As the slopes on both sides of this peak are big, there would be no dimer formation when the separation between two Fe monomers is above a. On the other hand, a dimer will be formed when the separation is below a. As we discussed above, the Fe atoms follow the random distribution function when they are deposited at low temperature. If we assume the average separation of the Fe atoms for a given coverage θ is r_θ then $r_\theta^2 \propto 1/\theta$. Following the rule of thumb for the random distribution function, one can derive the probability of forming dimers to be a^2/r_θ^2. This is supported by the kinetic Monte Carlo simulations, which yield that the dimer concentration of the system is linearly dependent on the coverage when the coverage is small.[24] For the formation of the superlattice, one needs to tune the coverage θ to satisfy the r_θ to be equal to the energy minimum position b. Therefore, the dimer concentration for the optimum coverage for forming the superlattice is proportional to a^2/b^2. In order to obtain a good quality superlattice, we need to limit the dimer formation that is to find the system with smaller a^2/b^2.

Table II shows the comparison of a^2/b^2 with the experimentally estimated dimer concentration for Fe/Cu(111) and Ce/Ag(111). One can find that the estimated values and the experimental data are quite similar. The deviation may come from the effect of the strain relaxation as discussed by Negulyaev *et al.*[25] From the table, one can also find that the dimer concentration for Fe/Cu(111) is much higher than the value for Ce/Ag(111). This could be the main reason for the different qualities of the superlattice in both systems. As Fe/Cu(111) forms a quasisuperlattice, one may speculate that the upper limit of a^2/b^2 for a good-quality superlattice formation is about 19%.

TABLE II. Comparison table of a^2/b^2 and the experimentally estimated dimer concentration for Fe/Cu(111) and Ce/Ag(111) systems. The data of Ce/Ag(111) is obtained from paper by Silly *et al.* (Ref. 1).

System	a (nm)	b (nm)	a^2/b^2 (%)	Dimer conc. (exp.) (%)
Fe/Cu(111)	0.5	1.1	19	24.7
Ce/Ag(111)	0.87	3.12	7.8	6.5

Besides the dimer formation during the deposition process, the dimer can also be induced if the annealing temperature is too high. For instance, we find there are noticeable increasing of Fe dimers on Cu(111) when the annealing temperature is above 14 K. This is due to the atoms can cross the repulsive energy barrier, E_r and form dimers with the assistance of the thermal energy. The two energy barriers, E_r and E_d set the upper and lower limit of the annealing temperature. It is good to have a system with E_r considerably larger than E_d.

To further demonstrate the proposed mechanism, we carried out kinetic Monte Carlo simulations for Fe/Cu(111) and Ce/Ag(111). For Fe on Cu(111), we use the interaction energy from the theoretical calculation by Stepanyuk *et al.*[22] We note that the calculated curve is almost the same as our measured data when the separation is larger than 0.7 nm. To separate the effects discussed above, we first artificially limit the dimer formation in the simulations. The effect of dimer formation will be discussed later. In order to show the effect of different E_i/E_d, we also artificially varied the diffusion barrier while keeping the same interaction energy. To simulate the experiments, we first deposited 4.5% MLE Fe atoms at 4 K with the deposition rate of 0.01 MLE/minute in the simulations. After that, we annealed the sample for 500 s. In order to obtain enough Fe hopping rates, we chose different annealing temperatures according to the respective diffusion barriers. In our case, the selection criterion is that there should be no significant difference for the samples annealed for 500 or 1000 s.

Figure 7(a)–7(c) presents the simulated results for three different diffusion barriers. When E_d=25 meV [Fig. 7(a)], 10 K is used as the annealing temperature. We can see that the simulation yields an excellent superlattice. The Fourier transform pattern of the image shows a sharp hexagonal pattern. We note that the E_i/E_d value corresponds to the values for Fe/Cu(111) and Ce/Ag(111) system. When E_d increase to 37.5 meV [Fig. 7(b)], we need to use the annealing temperature of 15 K to achieve enough hopping rates for Fe atoms with the given 500 s annealing time. We find some of the atoms start to deviate from the ideal positions. The Fourier transform pattern of the image still shows a hexagonal pattern but the spots are a little bit blurred, not as sharp as the spots shown in Fig. 7(a). When we further increase the diffusion barrier E_d to 50 meV [Fig. 7(c)], we use 20 K for the annealing temperature. We find that the hexagonal pattern disappears. The Fourier transform pattern only shows rings, indicating that the disorder is dominating even when the atoms have their preferred separation. The current ratio of

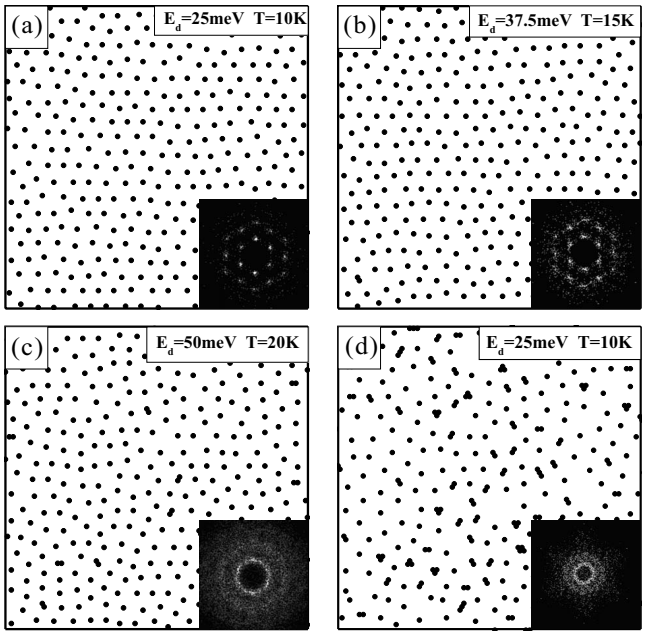

FIG. 7. Surface morphology of Fe adatoms on the Cu(111) surface obtained from KMC simulations. All the image sizes are 20 $\times 20$ nm^2. The same interaction energy is used all images. (a)–(c) exclude the dimer formation in the simulation and use 25, 37.5, and 50 meV as the diffusion barrier, respectively. (d) uses 25 meV diffusion barrier but also include the dimer formation.

E_i/E_d, 3.6% is approximately equivalent to the ratio in Fe/Ag(111) system. To summarize, in the absence of dimer formation, a ratio of E_i/E_d higher than $\approx$5% is required to obtain a good-quality superlattice. We note that we also used the interaction energy for Ce on Ag(111) and performed similar simulations. The same conclusion can be drawn.

Figure 7(d) presents the result of KMC simulations for E_d=25 meV and with the possibility for forming dimers/clusters. One can find that the dimers/clusters indeed strongly influence the superlattice formation. One can also find hexagonal structures in the region where a low concentration of dimer is found. This agrees well with our experimental findings (Fig. 6). The slight deviation may come from that the neglect of hopping of the dimer in the simulations. The barrier for dimer translation is typically between 1.5 and 2 times the diffusion barrier of the monomer.[30] When this is included, a better agreement is expected. In addition, the dimer is shown as a single object in the experimental images while it was plotted as two atoms in the simulated result, which may create different visual impressions.

V. CONCLUSION

In conclusion, we have studied the long-range interaction-mediated redistribution of Fe atoms on Ag(111) and Cu(111). It is found that Fe single atoms on Cu (111) form a quasi-hexagonal superlattice. For Fe on Ag(111), only disorderlike structures are found. In combination with the comparison several experimental systems and the kinetic Monte Carlo simulations the formation mechanisms of the superlattice are discussed. In order to obtain a good quality self-organized superlattice, two basic requirements need to be fulfilled: the ratio of the interaction energy E_i versus the diffusion barrier E_d needs to be larger than $\approx$5% and the square of the repulsive ring radius a relative to the superstructure lattice constant b needs to be smaller than $\approx$19%.

ACKNOWLEDGMENTS

This work is supported by NSFC (Grants No. 10604026, No. 10834001, No. 10874076, and No. 10974087), NCET and the State Key Programme for Basic Research of China (Grants No. 2007CB925104 and No. 2010CB923401).

*Corresponding author; hfding@nju.edu.cn

[1] F. Silly, M. Pivetta, M. Ternes, F. Patthey, J. P. Pelz, and W.-D. Schneider, Phys. Rev. Lett. **92**, 016101 (2004).
[2] F. Silly, M. Pivetta, M. Ternes, F. Patthey, J. P. Pelz, and W.-D. Schneider, New J. Phys. **6**, 16 (2004).
[3] P. Gambardella, A. Dallmeyer, K. Maiti, M. C. Malagoli, S. Rusponi, P. Ohresser, W. Eberhardt, C. Carbone, and K. Kern, Phys. Rev. Lett. **93**, 077203 (2004).
[4] H. J. Elmers, J. Hauschild, H. Höche, U. Gradmann, H. Bethge, D. Heuer, and U. Köhler, Phys. Rev. Lett. **73**, 898 (1994).
[5] P. Gambardella, A. Dallmeyer, K. Maiti, M. C. Malagoli, W. Eberhardt, K. Kern, and C. Carbone, Nature (London) **416**, 301 (2002).
[6] N. Knorr, H. Brune, M. Epple, A. Hirstein, M. A. Schneider, and K. Kern, Phys. Rev. B **65**, 115420 (2002).
[7] J. Shen, R. Skomski, M. Klaua, H. Jenniches, S. S. Manoharan, and J. Kirschner, Phys. Rev. B **56**, 2340 (1997).
[8] Y. Mo, K. Varga, E. Kaxiras, and Z. Zhang, Phys. Rev. Lett. **94**, 155503 (2005).
[9] H. F. Ding, V. S. Stepanyuk, P. A. Ignatiev, N. N. Negulyaev, L. Niebergall, M. Wasniowska, C. L. Gao, P. Bruno, and J. Kirschner, Phys. Rev. B **76**, 033409 (2007).
[10] M. F. Crommie, C. P. Lutz, and D. M. Eigler, Science **262**, 218 (1993).
[11] H. C. Manoharan, C. P. Lutz, and D. M. Eigler, Nature (London) **403**, 512 (2000).
[12] J. Repp, F. Moresco, G. Meyer, K.-H. Rieder, P. Hyldgaard, and M. Persson, Phys. Rev. Lett. **85**, 2981 (2000).
[13] J. Koutecký, Trans. Faraday Soc. **54**, 1038 (1958).
[14] T. B. Grimley, Proc. Phys. Soc. **90**, 751 (1967).
[15] K. H. Lau and W. Kohn, Surf. Sci. **75**, 69 (1978).
[16] T. L. Einstein and J. R. Schrieffer, Phys. Rev. B **7**, 3629 (1973).
[17] T. T. Tsong, Phys. Rev. B **6**, 417 (1972).
[18] T. T. Tsong, Phys. Rev. Lett. **31**, 1207 (1973).
[19] P. Hyldgaard and M. Persson, J. Phys.: Condens. Matter **12**, L13 (2000).

[20] N. N. Negulyaev, V. S. Stepanyuk, L. Niebergall, P. Bruno, M. Pivetta, M. Ternes, F. Patthey, and W.-D. Schneider, Phys. Rev. Lett. **102**, 246102 (2009).

[21] H. Brune, in *Superlattices of Atoms, Molecules and Islands in Properties of Single Organic Molecules on Crystal Surfaces*, edited by F. Rosei, P. Grütter, and W. Hofer (Springer, New York, 2006), pp. 247–267.

[22] V. S. Stepanyuk, L. Niebergall, R. C. Longo, W. Hergert, and P. Bruno, Phys. Rev. B **70**, 075414 (2004).

[23] N. N. Negulyaev, V. S. Stepanyuk, L. Niebergall, W. Hergert, H. Fangohr, and P. Bruno, Phys. Rev. B **74**, 035421 (2006).

[24] J. Hu, B. Teng, F. Wu, and Y. Fang, New J. Phys. **10**, 023033 (2008).

[25] N. N. Negulyaev, V. S. Stepanyuk, L. Niebergall, P. Bruno, W. Auwärter, Y. Pennec, G. Jahnz, and J. V. Barth, Phys. Rev. B **79**, 195411 (2009).

[26] S. Ovesson, A. Bogicevic, G. Wahnström, and B. I. Lundqvist, Phys. Rev. B **64**, 125423 (2001).

[27] G. Ehrlich and F. Watanabe, Langmuir **7**, 2555 (1991).

[28] J. Kirschner, H. Engelhard, and D. Hartung, Rev. Sci. Instrum. **73**, 3853 (2002).

[29] N. N. Negulyaev, V. S. Stepanyuk, W. Hergert, H. Fangohr, and P. Bruno, Surf. Sci. **600**, L58 (2006).

[30] H. Brune, Surf. Sci. Rep. **31**, 121 (1998).